Shifting the boundaries: pulse-shape effects in the atom-optics kicked rotor

P. H. Jones, M. Goonasekera, H. E. Saunders-Singer & D. R. Meacher*
Department of Physics and Astronomy, University College London, Gower Street, London, United Kingdom, WC1E 6BT

We present the results of experiments performed on cold caesium in a pulsed sinusoidal optical potential created by counter-propagating laser beams having a small frequency difference in the laboratory frame. Since the atoms, which have average velocity close to zero in the laboratory frame, have non-zero average velocity in the co-moving frame of the optical potential, we are able to centre the initial velocity distribution of the cloud at an arbitrary point in phase-space. In particular, we demonstrate the use of this technique to place the initial velocity distribution in a region of phase-space not accessible to previous experiments, namely beyond the momentum boundaries arising from the finite pulse duration of the potential. We further use the technique to explore the kicked rotor dynamics starting from a region of phase-space where there is a strong velocity dependence of the diffusion constant and quantum break time and demonstrate that this results in a marked asymmetry in the chaotic evolution of the atomic momentum distribution.

PACS numbers: 32.80.Pj

INTRODUCTION

Classical systems with chaotic dynamics can exhibit very different behavior in the quantum regime. One such system that has been widely studied is the delta-kicked-rotor (DKR) [1], realized using laser-cooled atoms in a periodic optical potential, or optical lattice [2]. These experiments have shown the difference between the quantum DKR and its classical counterpart by demonstrating purely quantum mechanical phenomena such as dynamical localization (the quantum suppression of classical momentum diffusion) [3] and quantum resonances (ballistic rather than diffusive energy growth) [4]. More recent theoretical [5] and experimental work [6] has shown that by breaking temporal symmetry a fully chaotic 'ratchet' may be achieved by imposing a momentum dependence on the momentum diffusion coefficient. In the present work we show how the modulation of the diffusion coefficient that unavoidably arises in a real experiment due to the finite temporal width of the kicks [7] can also be exploited to produce a strongly asymmetric momentum diffusion around a non-zero momentum. To explore this we introduce a moving optical potential so that in the laboratory frame the atomic momentum distribution may be centered at an arbitrary location in phase space, including regions inaccessible to previous experiments that use a stationary potential.

An optical lattice formed by two counter-propagating laser beams may be used to trap laser-cooled atoms in a one-dimensional periodic potential [8]. If the laser beams, wavelength λ ($k_L = 2\pi/\lambda$), are pulsed with period T then the atomic Hamiltonian is

$$H = \frac{p^2}{2M} + V_0 \cos(2k_L x) \sum F(t - nT) \qquad (1)$$

where p is the atomic momentum, M the mass, V_0 the optical potential depth and $F(t)$ a square pulse centered at $t = 0$ of width t_p. If the co-ordinates are re-scaled to a dimensionless form then the correspondence with the DKR becomes clear:

$$\mathcal{H} = \frac{\rho^2}{2} + k \cos(\phi) \sum f(\tau - n) \qquad (2)$$

where $\phi = 2k_L x$ is a scaled (dimensionless) position, $\rho = 4\pi T p/M\lambda$ a scaled momentum, $\tau = t/T$ a scaled time and $\mathcal{H} = (4k_L^2 T^2/M)H$. The function $f(\tau)$ is now a square pulse of unit amplitude with duration $\eta = t_p/T$ ($\ll 1$) and $k = (8V_0/\hbar)\omega_R T^2$ (with ω_R the recoil frequency) the scaled kick strength. The scaled unit of system action, or effective Planck constant $\hbar_{eff}$, may be found by evaluating the commutator $[\phi, \rho] = i8\omega_R T = i\hbar_{eff}$ and is thus controllable through the period of the kicking cycle. The ability of control the magnitude of $\hbar_{eff}$ therefore makes the DKR an important system in the study of chaotic dynamics. For the case of finite temporal width kicks the kick strength is modified to become $K = (t_p/T)k = (V_0/\hbar) \times t_p \times \hbar_{eff}$, known as the stochasticity parameter. For the classical DKR the dynamics are governed entirely by this single parameter K. As K is increased from zero stable trajectories start to break up: at $K \simeq 1$ the last stable trajectory that inhibits momentum diffusion is broken, and for $K > 4$ the phase space is globally chaotic and the momentum grows diffusively and without limit [9]. An experimental study of momentum diffusion in 'mixed' phase spaces where both stable and chaotic dynamics are present using similar techniques to those outlined in this paper will be the subject of a future publication [10]. In the quantum case the parameter $\hbar_{eff}$ is also important as this determines the time for which the momentum will grow (the break time $t^* \propto K^2/\hbar_{eff}^2$) before the quantum interference phenomenon of dynamical localization suppresses further increase.

From the above it would seem that the transition to global chaos that occurs with increasing $K \propto t_p$ may be studied by simply increasing the duration of the pulses.

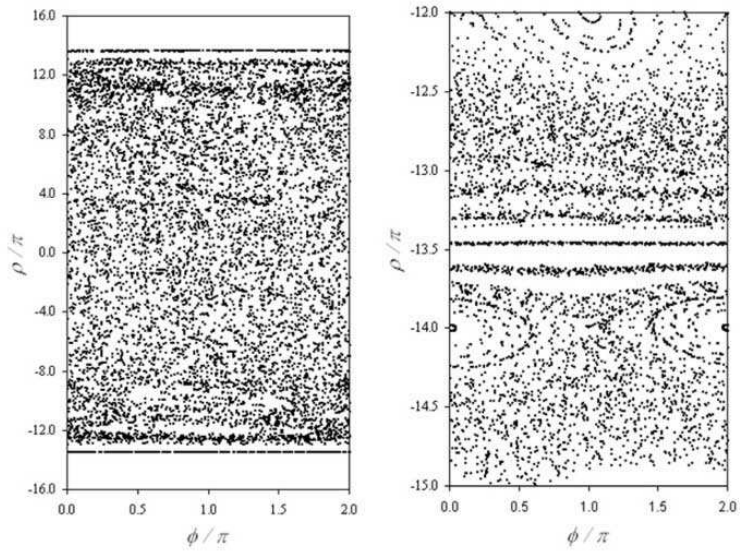

FIG. 1: Phase Space diagrams for $K(\rho = 0) = 5.3$, 120 kicks. Left: For a momentum boundary at $\pm 13.5\pi$ all trajectories that start within this region remain within the momentum boundaries. Right: Trajectories starting both side of the momentum boundary shows stable motion in the region of $\rho = \rho_b$.

In fact, outside the limit $\eta \ll 1$ the finite width of the pulses has a significant effect on the momentum diffusion. This can be understood with the semiclassical picture of an atom moving a finite distance during the time t_p when the potential is switched on. The momentum kick received by the atom is then averaged over the time t_p, such that for all momenta greater than zero the kick is less than that imparted by a δ-function pulse. A consequence of this is the occurrence of a *momentum boundary* at a particular momentum where the atom travels one period of the potential during t_p, and the momentum transferred is averaged to zero over the pulse. The momentum at which this occurs is thus $p_b = \pm M\lambda/2t_p$, or in dimensionless (scaled) units:

$$\rho_b = \pm \frac{M\lambda^2}{8\pi\hbar t_p}\hbar_{eff}. \tag{3}$$

In [7] it was shown that the resulting dependence of the stochasticity parameter on momentum, $K_{eff}(\rho)$, could be related to the shape of the pulse through a Fourier transform, and so for the square pulse $f(\tau)$ considered above:

$$K_{eff}(\rho) = K\frac{\sin(\pi\rho/\rho_b)}{\pi\rho/\rho_b}, \tag{4}$$

where the first zeroes of $K_{eff}(\rho)$ are as given by equation 3.

The momentum boundaries are visible in a phase space diagram or Poincaré section as shown in figure 1. The left hand side of this diagram was obtained by iterating the well-known Standard Map (setting T=1 w.l.o.g.):

$$\phi_{n+1} \;=\; \phi_n + \rho_n; \tag{5}$$

$$\rho_{n+1} \;=\; \rho_n + K\sin\phi_{n+1}, \tag{6}$$

but replacing K with $K_{eff}(\rho_n)$. The momentum boundary was set to be $\rho_b = 42.5 = 13.5\pi$ and all trajectories were started within $\rho = \pm\rho_b$. The peak value of K was 5.3, and the map was iterated through 120 kicks. As can be seen all the trajectories remain bounded within $\rho = \pm\rho_b$, as once an atom has reached this momentum the stochasticity parameter, and hence the diffusion constant $D \propto K^2/2$ (to lowest order, higher order corrections arise from correlations between kicks [9, 11]) , has dropped to zero and the momentum does not change.

The region around $\rho = -13.5\pi$ is shown in greater detail in the right hand side of the figure for the same parameters as above, but with trajectories starting both sides of the momentum boundary. This helps to show the the stable region around ρ_b as the unbroken line at $\rho = -13.5\pi$ corresponds to uniform motion at constant momentum, whereas the regions at slightly larger and smaller momenta show chaotic dynamics where diffusive momentum growth is expected.

EXPERIMENT

For our quantum chaos experiments we use a cloud of cesium atoms captured from the background vapor in a standard 6-beam magneto-optic trap and further cooled in an optical molasses to an rms dimensionless momentum width of $\sigma_\rho \simeq 4$. The atoms are released by switching off the molasses beams with an acousto-optic modulator (AOM) and the sinusoidal 'kicking' potential applied. This is formed from two horizontal counter-

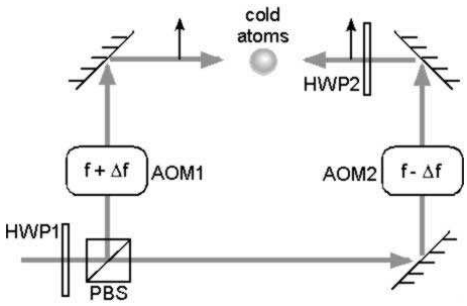

FIG. 2: Diagram of apparatus. The half-wave plate (HWP1) and polarizing beam splitter (PBS) split the beam into two equal intensity parts. The acousto-optic modulators AOM1 and AOM2 shift the frequencies by $f \pm \Delta f$. The half-wave plate HWP2 is used to set the polarizations parallel.

propagating beams from a titanium sapphire (Ti:S) laser, maximum output power 1W at 852nm, detuned several thousand linewidths below the D2 cooling transition in cesium. At these very large detunings the spontaneous scattering rate is negligible. The short pulses required for the kicks are created by an arbitrary function generator, the output of which is used to trigger an AOM via a fast rf switch. After kicking the cloud of atoms is allowed to expand ballistically for a few milliseconds before a pair of counter-propagating near-resonant laser beam is switched on and the fluorescence imaged on a cooled CCD camera. From the spatial distribution of the fluorescence it is thus possible to extract the momentum distribution.

In order to investigate the momentum dependence of the diffusion constant caused by the finite width of the kicks it is necessary to have a sample of atoms with a narrow momentum distribution centered at a non-zero momentum, such as may be prepared by laser cooling in a uniform magnetic field [12]. A disadvantage of this technique is the the moving cloud of cold atoms quickly reaches the edge of the field of view of the CCD camera, limiting in practise the range of momenta it is possible to investigate. Instead we have used a moving optical lattice created by laser beams with different frequencies in the laboratory frame such that in the rest frame of the lattice the cloud of atoms has a non-zero mean momentum. The apparatus for this experiment is shown in figure 2. The output from the Ti:S laser is split into two equal intensity beams using a half-wave plate and polarizing beam splitter. These beams are then passed through separate AOMs driven by separate phase-locked radio-frequency generators at a frequency $f = 80$MHz. A single arbitrary function generator is used to trigger both AOMs via separate switches. A second half-wave plate is used to set the polarizations parallel. If a frequency difference $2\Delta f$ is imposed on the kicking beams as shown in figure 2 the the resulting interference pattern moves at a velocity $(\lambda\Delta f)\mathrm{ms}^{-1}$, giving a scaled momentum in the frame of the moving optical lattice of $\rho_L = M\lambda^2\Delta f\hbar_{eff}/4\pi\hbar$. Using this technique it is possible to vary the starting momentum of the cold atoms in the frame of the potential continuously over a large range before the kicking beams become significantly misaligned from the cloud. In our experiment the effect of misalignment becomes noticeable at around $\Delta f = 1$MHz, or $\rho_L \simeq 120$ for $\hbar_{eff}$=1.

Using this apparatus we have checked that dynamical localization occurs when using short ($\eta \ll 1$) pulses, and that when longer pulses are used we can observe the effects of the momentum boundary as a sharp drop in the momentum distribution at approximately the momentum calculated from equation 3. In order to investigate the effects of the boundary on diffusion we perform an experiment for the same parameters as the phase space diagrams of figure 1, i.e. $K = 5.3$ (10% error arising mainly from the measurement of the beam intensity), with $t_p = (1.42 \pm 0.02)\mu$s and $T = (9.47 \pm 0.02)\mu$s so that $\hbar_{eff}$ =1, $\eta = 0.15$ and $\rho_b = 42.5$. The momentum in the lattice frame was varied between 0 and 73 in order to explore the region past ρ_b. For each measurement of the momentum distribution an average of five images was taken.

RESULTS

Figure 3 shows some typical results taken with a moving lattice as described above. The solid black line is the momentum distribution when no kicking is applied. The light grey dashed line is that for $\Delta f = 0$, i.e. a stationary lattice ($\rho_L = 0$). This is (almost) symmetric about $\rho = 0$, any slight deviation probably being due to a misalignment of the kicking beams. The grey dotted line is for $\rho_L = 29$ and shows a very large asymmetry towards negative momenta due to the large gradient of diffusion coefficient at $\rho = 29$. The diffusion coefficient falls to zero at $\rho_L = 42.5$ on the more positive momentum side of the distribution, forming an effective barrier to diffusion. On the lower momentum side the diffusion coefficient is higher and there is a greater region of phase space available to diffuse into. This effect is enhanced by the variation in the break time ($t^* \propto K^2 \propto D$) across

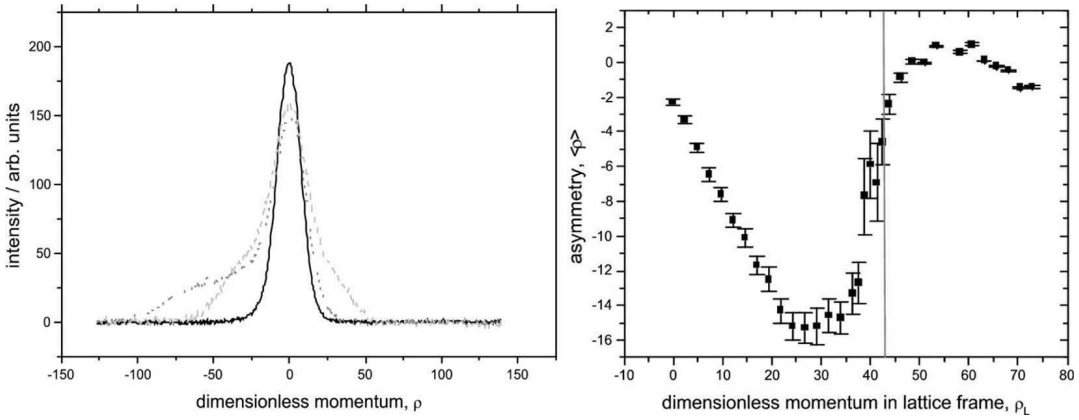

FIG. 3: Results of kicked rotor experiment with a moving lattice. Left: Momentum distributions for different values of starting momentum in the moving lattice frame. Heavy black line: no kicks. Light grey dashed line: $\rho_L = 0$. Grey dotted line: $\rho_L = 29$, a large asymmetry has accumulated to more negative momenta. Right: Graph of asymmetry of the momentum distribution vs starting momentum in the moving lattice frame. The vertical grey line indicated the calculated position of the momentum boundary.

this region - smaller to the higher momentum side so energy is absorbed slowly for a short time, and larger to the negative momentum side.

We characterize the amount of asymmetry by calculating the first moment of the momentum distribution, by $\langle\rho\rangle = \int \rho N(\rho)d\rho / \int N(\rho)d\rho$ and plotting as a function of ρ_L. Results are shown in figure 3. For increasing ρ_L a large negative asymmetry can be seen to increase from the $\rho_L = 0$ value as the diffusion to positive momenta becomes restricted by the presence of the momentum boundary (the location of which is shown as a vertical grey line in figure 3). Past this value of momentum is the area of phase space inaccessible to conventional experiments that use a static potential. By starting at a momentum just past the boundary we see a small growth in momentum as K is small but non-zero, and an asymmetry of the opposite sense to that before the boundary begin to accumulate. The magnitude of this asymmetry is less due both to the smaller diffusion constant and smaller break time in this region because of the modulation of $K_{eff}(\rho)$ imposed by the finite width of the kicks but of an opposite sign due to an opposite sign gradient of diffusion coefficient.

In conclusion, we have demonstrated that the finite width of the pulses used in a kicked rotor experiment can have a significant effect. By introducing a moving optical potential we have been able to exploit the gradient of diffusion coefficient to produce a strongly asymmetric momentum diffusion. Using the moving potential has also enabled us to investigate diffusion in the regions of phase space beyond the momentum boundaries imposed by the finite kicks that are not otherwise accessible. In the future we intend to use the moving potential technique to study the effect on chaotic momentum diffusion of engineered pulse shapes and sequences, or to selectively prepare cold atoms in stable islands of a mixed phase space [13].

We would like to thank Tania Monteiro and the UCL Quantum Chaos Group for useful discussions, and EPSRC for financial support.

* philip.jones@ucl.ac.uk; http://lasercooling.phys.ucl.ac.uk

[1] A. L. Lichtenberg and M. A. Lieberman, *Regular and Chaotic Dynamics*, (Springer-Verlag, Berlin, 1991).
[2] F. L. Moore, J. C. Robinson, C. F. Barucha, Bala Sundaram and M. G. Raizen, Phys. Rev. Lett., **75** 4598 (1995).
[3] C. T. Bharucha, J. C. Robinson, F. L. Moore, Bala Sundaram, Qian Niu and M. G. Raizen, Phys. Rev. E, **60** 3881 (1999).
[4] W. H. Oskay, D. A. Steck, V. Milner, B. G. Klappauf and M. G. Raizen, Opt. Commun., **179** 137 (2000).
[5] T. Jonckheere, M. R. Isherwood and T. S. Monteiro, e-print nlin/0304036
[6] P. H. Jones, M. Goonasekera, H. E. Saunders-Singer and D. R. Meacher, e-print quant-ph/0309149 (2003)
[7] B. G. Klappauf, W. H. Oskay, D. A. Steck and M. G. Raizen, Physica D, **131** 78 (1999).
[8] D. R. Meacher, Contemp. Phys., **39** 329 (1998).
[9] B. G. Klappauf, W. H. Oskay, D. A. Steck and M. G. Raizen Phys. Rev. Lett., **81** 4044 (1998).
[10] M. Goonasekera, P. H. Jones, H. E. Saunders-Singer and D. R. Meacher. Manuscript in preparation.
[11] A. B. Rechester and R. B. White. Phys. Rev. Lett., **44** 1586 (1980)
[12] S.-Q. Shang, B. Sheehy, P. van der Straten, and H. Metcalf. Phys. Rev. Lett., **65** 317 (1990)
[13] W. K. Hensinger, N. R. Heckenberg, G. J. Milburn and H. Rubinstein-Dunlop. J. Opt. B Quantum Semiclass. Opt., **5** R83 (2003)